*Progress In Electromagnetics Research, PIER 39, 147–175, 2003*

# SIMPLE TIME-DOMAIN EXPRESSIONS FOR PREDICTION OF CROSSTALK ON COUPLED MICROSTRIP LINES

**C. C. Chai, B. K. Chung, and H. T. Chuah**

Faculty of Engineering
Multimedia University
Jalan Multimedia
63100 Cyberjaya, Selangor, Malaysia

**Abstract**—This paper presents an improved variant of time-domain method for predicting crosstalk on parallel-coupled matched terminated microstrip lines. This method derives simple near-end and far-end time-domain crosstalk expressions which are applicable to lossless case with significant harmonic frequency $< 1\,\text{GHz}$. The expressions are in polynomial form with geometrical dimensions of the structure and stimulus information as the only required entry parameters. They are simpler as compared to other methods because the difficult-to-determine distributed $RLCG$ electrical parameters of the coupled lines are not needed. A look-up table for the polynomial coefficients is generated for easy application of this technique. The expressions are applicable for board thickness of 4–63 mils, 30–70 $\Omega$ line characteristic impedance, $0.5W$–$4.0W$ (where $W$ is the line width) inner edge to edge separation, and 3–5 dielectric constant. For significant harmonic frequency $> 1\,\text{GHz}$, the effect of both losses and dispersion on the crosstalk levels is accounted for by investigating the gradient of the distorted driving signal. The peak crosstalk levels are then predicted by modifying the time derivative term in the lossless expressions. In addition, the far-end crosstalk is proved to saturate at half of the magnitude of the driving signal entering the active line. The saturation phenomenon is studied from the viewpoint of difference in odd-mode and even-mode propagation velocities.

## 1 Introduction

## 2 The Proposed Simple Time-Domain Crosstalk Expressions

2.1 Determination of the Polynomial Coefficients
2.2 Deviation Analysis

**3 Saturation of the Far-end Crosstalk**

**4 The Effect of Losses and Dispersion on Crosstalk Noise**
4.1 The Valid Frequency Range for Lossless and Dispersionless Assumption
4.2 Incorporation of Losses and Dispersion Effect in Far-end Crosstalk Prediction

**5 Procedure for Prediction of Crosstalk**

**6 Comparisons with Results from Field Solver and other Models**

**7 Comparisons with Measurement Results**

**8 Conclusion**

**References**

## 1. INTRODUCTION

The printed circuit board cost is generally proportional to the number of layers and board surface area. The layout engineers will always try to use the fewest number of layers and smallest board surface area that will do the job. However, very dense designs cause more closely spaced traces, consequently yields more crosstalk. Thus, pre-layout crosstalk analysis is essential so as to find a tradeoff between routing density and signal integrity. These factors have motivated the researchers to propose simple, efficient and accurate crosstalk analysis methods with minimum mathematical details for fast prediction of crosstalk noises.

Reference [1] has presented expressions (1) and (2) which can estimate both near-end and far-end time-domain crosstalk waveforms for lossless case:

$$V_{ne}(t) = \frac{1}{4}\left(\frac{C_m}{C_t} + \frac{L_m}{L_s}\right) \cdot [V_s(t) - V_s(t - 2T_p)] \tag{1}$$

$$V_{fe}(t) = \frac{1}{2}\left(\frac{C_m}{C_t} - \frac{L_m}{L_s}\right) \cdot T_p \cdot \frac{dV_s(t - T_p)}{dt} \tag{2}$$

The voltages and currents induced along the line due to both mutual inductive and capacitive couplings are calculated and then summed by applying the principle of superposition. This method has the advantage of giving fast quantitative estimations of crosstalk noises provided the

per-unit-length (p.u.l.) inductance and capacitance parameters could be calculated quickly.

Reference [2] provided simple expressions for crosstalk estimations, in terms of separation distance between traces (centre to centre) and trace height from the reference plane. However, the line width and the dielectric material around the traces are not included in the expressions. In addition, the expression does not calculate the near-end and far-end crosstalk values separately.

Reference [3] provided empirical expressions for total- and mutual-capacitances ($C_t, C_m$), and self- and mutual- inductances ($L_s, L_m$) for parallel-coupled microstrip lines. Assuming matched terminations at each ends of the lines, the $L_s, L_m, C_t, C_m$ values can be substituted into expressions (1) and (2) to estimate crosstalk. However, the derived expressions for the capacitances and inductances are too complicated for hand calculations.

The purpose of this paper is to propose simple and accurate time-domain expressions for estimating the near-end and far-end crosstalk on parallel-coupled matched terminated microstrip lines. The proposed expressions are similar to expressions (1) and (2), but the capacitance and inductance terms are replaced by simple polynomial expressions with geometrical dimensions of the structure as the only required entry parameters. While compared to Reference [2], the proposed equations are more complete where the substrate dielectric material has been taken into account and the near-end and far-end crosstalk values are calculated separately. The proposed expressions are suitable for hand calculations and applicable for a wide range of practical trace dimensions and dielectric materials. The validity of this work is verified by comparisons with measured values, simulation results generated from commercial software and those available in literature.

## 2. THE PROPOSED SIMPLE TIME-DOMAIN CROSSTALK EXPRESSIONS

The proposed simple time-domain near-end and far-end crosstalk expressions for parallel coupled microstrip lines (Figure 1) are in the following form:

$$V_{ne}(t) = \frac{V_s(t) - V_s(t - 2T_p)}{P_{ne3}\left(\frac{S}{H}\right)^3 + P_{ne2}\left(\frac{S}{H}\right)^2 + P_{ne1}\left(\frac{S}{H}\right) + P_{ne0}} \tag{3}$$

$$V_{fe}(t) = \frac{T_p \cdot [dV_s(t - T_p)/dt]}{P_{fe3}\left(\frac{S}{H}\right)^3 + P_{fe2}\left(\frac{S}{H}\right)^2 + P_{fe1}\left(\frac{S}{H}\right) + P_{fe0}} \tag{4}$$

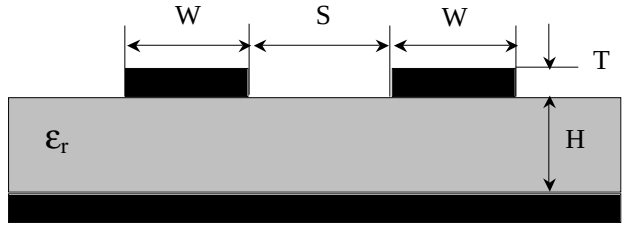


**Figure 1.** Cross-section of a pair of parallel-coupled microstrip lines.

where $V_{ne}(t)$, $V_{fe}(t)$, $V_s(t)$, and $T_p$ are the near-end crosstalk, far-end crosstalk, source voltage, and propagation time along the coupled length respectively.

Our intention is to provide a look-up table consisting of a few sets of polynomial coefficients. Each set of coefficients is applicable to specific ranges of $\varepsilon_r$, $\frac{W}{H}$ and $\frac{S}{W}$. The derived coefficients can predict crosstalk on parallel-coupled microstrip lines of the following parameters:

- microstrip line characteristic impedance $Z_0$ at discrete values of $30\,\Omega$, $40\,\Omega$, $50\,\Omega$, $60\,\Omega$ and $70\,\Omega$ (for loosely coupled lines where $L_m \ll L_s$ and $C_m \ll C_t$, the characteristic impedance of the line is not altered significantly by the presence of the adjacent line, therefore $Z_0$ can be approximated by that of a single line);
- substrates with dielectric constants $\varepsilon_r$ ranges from 3.0 to 5.0 (e.g., BT, CEM1/CEM3, Cynate Ester, Kevlar, FR4-epoxy, Polyamide, Polyimide, etc.);
- substrate thickness $H$ ranges from 4 to 63 mils (the applicable range of $W$ depends on $H$ and $\varepsilon_r$ since the characteristic impedance is a function of both $W/H$ and $\varepsilon_r$);
- $S/W$ from 0.5 to 4.0

A method to incorporate the high frequency conductor and dielectric losses, and dispersion effect in crosstalk analysis is also proposed in Section 4.2.

Similar approach can be found in [4], where a look-up table for capacitive crosstalk coupling of coupled microstrip lines in frequency domain for $Z_0 = 50\,\Omega$, $90\,\Omega$ and $120\,\Omega$ is provided. While Reference [5] provided graphs for backward (near-end) coupling coefficients of coupled lines in a homogeneous medium. The author found the need to provide a simpler and more complete look-up table that cover a wide range of practical board parameters.

The proposed expressions can be used to plot the time-domain waveform of the near-end and far-end crosstalk. This is useful in

investigating the time intervals during which the coupled noise on a specific signal line can affect the functioning of a system [6].

### 2.1. Determination of the Polynomial Coefficients

The polynomial coefficients in expressions (3) and (4) are obtained by applying curve-fitting on Ansoft's Maxwell Spicelink simulation results. Consider two $50\,\Omega$ parallel-coupled matched terminated microstrip lines with $W = 10\,\text{mils}$, $H = 6\,\text{mils}$, $\varepsilon_r = 4.5$, and coupled length $l = 15\,\text{cm}$. The typical value of 1 ounce is used for the trace thickness $T$. The input signal is a step voltage with $5\,\text{V}$ amplitude and $2\,\text{ns}$ rise time $T_r$. The near-end crosstalk expression can be rewritten in the following form:

$$V_{ne}(t) = k \cdot \frac{V_s(t) - V_s(t - 2T_p)}{P\left(\frac{S}{H}\right)} \tag{5}$$

where both polynomial $P\left(\frac{S}{H}\right)$ and constant $k$ are to be determined.

The propagation time $T_p$ along the coupled length $l$ can be estimated by first calculating the effective dielectric constant [7] from Equation (6):

$$\varepsilon_{eff} = 1 + \frac{(\varepsilon_r - 1)}{2} \cdot \left[1 + \frac{1}{\sqrt{1 + 10\frac{H}{W}}}\right] \tag{6}$$

$T_p$ is then calculated as

$$T_p = \frac{l}{(c/\sqrt{\varepsilon_{eff}})} \tag{7}$$

where $l$ and $c$ are the coupled length and the speed of light in vacuum respectively.

In this example, $2T_p = 1.85\,\text{ns} < T_r = 2\,\text{ns}$, therefore it is a short-coupled line. From Equation (5), the peak near-end voltage of a short-coupled line is given by

$$V_{ne_{peak}} = \frac{k}{P\left(\frac{S}{H}\right)} \cdot \frac{2T_p}{T_r} \cdot V_0 \tag{8}$$

Maxwell Spicelink is used to simulate crosstalk of the coupled lines. The peak values of the near-end crosstalk are recorded for $S$ ranges from $0.25W$ to $4.0W$. Graph of near-end crosstalk versus $\frac{S}{H}$ is then

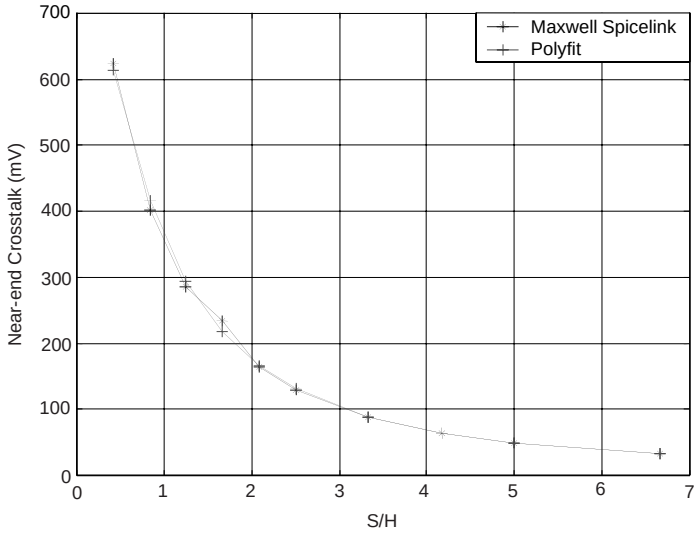


**Figure 2.** Polyfitting near-end crosstalk versus $S/H$.

plotted. Subsequently, the *polyfit function* available in Matlab is used to find the coefficients of a polynomial $P\left(\frac{S}{H}\right)$ that fits the graph in a least-squares means. It is found that the following polynomial of degree 3 is sufficient to reproduce the curve accurately (see Figure 2):

$$P\left(\frac{S}{H}\right) = -0.00947 \cdot \left(\frac{S}{H}\right)^3 + 0.5728 \cdot \left(\frac{S}{H}\right)^2 + 1.2997 \cdot \left(\frac{S}{H}\right) + 0.9080 \tag{9}$$

From Equations (8) and (9), the average value of constant $k$ can be determined. Rearrange terms to eliminate $k$ produce the proposed near-end crosstalk in form of expression (3) with:

$$P_{ne3} = -0.0437, \quad P_{ne2} = 2.65, \quad P_{ne1} = 6.00, \quad P_{ne0} = 4.19$$

## 2.2. Deviation Analysis

Deviation analysis is carried out to investigate the accuracy of the proposed expressions as compared to those of commercial software. Ansoft's 2D Extractors is used for the comparison purpose.

Since the proposed expressions in (3) and (4) are similar to expressions (1) and (2), except the capacitance and inductance terms are replaced by simple polynomial expressions in term of $\frac{S}{H}$, the

deviations of the predicted near-end crosstalk values can be studied by comparing the values of $\frac{1}{4}\left(\frac{C_m}{C_t}+\frac{L_m}{L_s}\right)$ calculated using 2D Extractors with the values of polynomial $P_{ne3}\left(\frac{S}{H}\right)^3+P_{ne2}\left(\frac{S}{H}\right)^2+P_{ne1}\left(\frac{S}{H}\right)+P_{ne0}$.

The deviation analysis is performed within the region of $4.0 \leq \varepsilon_r \leq 5.0$, $4\,\text{mils} \leq H \leq 8\,\text{mils}$, and $0.5 \leq S/W \leq 4.0$ (the point selected for derivation of the polynomial coefficients is located around the centre of this region). The characteristic impedance of any arbitrary coupled line chosen for deviation analysis is maintained at $50\,\Omega$. In this case, the maximum crosstalk deviation is determined to be 13.60%.

Similar procedure is repeated to derive sets of coefficients that apply to other ranges of $\varepsilon_r$, $H$, $Z_0$ and $\frac{S}{W}$. A look-up table is constructed as shown in Table 1. The sets of polynomial coefficients for the far-end crosstalk and the deviation analysis are determined and performed in the similar manner.

## 3. SATURATION OF THE FAR-END CROSSTALK

The proposed far-end crosstalk expression in (4) can be used directly provided saturation does not occur. In this section, we will prove that the far-end crosstalk saturates at half of the magnitude of the driving signal entering the active line.

Letting

$$K_f = \frac{1}{P_{fe3}\left(\frac{S}{H}\right)^3 + P_{fe2}\left(\frac{S}{H}\right)^2 + P_{fe1}\left(\frac{S}{H}\right) + P_{fe0}}$$

where $K_f$ is the forward crosstalk coefficient, Equation (4) can be re-written as:

$$V_{fe}(t) = K_f \cdot T_p \cdot [dV_s(t - T_p)/dt] \tag{10}$$

Equation (10) reveals that the far-end crosstalk depends on the time derivative of the driving signal at one propagation time earlier. This implies that $V_{fe}$ increases as $T_r$ decreases. It is observed that the far-end crosstalk will saturate as $T_r$ is reduced to a very small value. This phenomenon, which is seldom discussed in literature, can be explained by decomposing the wave into even- and odd-mode.

Consider a pair of coupled transmission lines as depicted in Figure 3. This arrangement may be analyzed by first considering excitation under even-mode conditions alone, then odd-mode conditions alone, and finally combining the results. The notation is given in Figure 4. It is assumed that losses and dispersion effect may be neglected so that the propagation constant, $\gamma = \alpha + j\beta$, reduces to the

**Table 1.** Look-up table for near-end and far-end crosstalk coefficients.

| $\varepsilon_r$ | Applicable Range | | | Near-end Crosstalk Coefficients | | | | | Far-end Crosstalk Coefficients | | | | |
|---|---|---|---|---|---|---|---|---|---|---|---|---|---|
| | $H$/mils | $Z_0$ | $S/W$ | $P_{ne3}$ | $P_{ne2}$ | $P_{ne1}$ | $P_{ne0}$ | Worst-case Deviation* | $P_{fe3}$ | $P_{fe2}$ | $P_{fe1}$ | $P_{fe0}$ | Worst-case Deviation* |
| $3.0 \leq \varepsilon_r < 4.0$ | 4–8 | 30 | 0.5–4.0 | 0.0093 | 0.825 | 14.52 | −2.77 | 18.41% | 0.0031 | −1.11 | −6.78 | −16.47 | 14.17% |
| | | 40 | 0.5-4.0 | −0.0222 | 1.86 | 7.20 | 5.94 | 13.63% | 0 | −1.25 | −6.18 | −13.09 | 16.55% |
| | | 50 | 0.5-4.0 | −0.0482 | 2.31 | 6.16 | 4.27 | 14.36% | 0 | −1.45 | −5.15 | −12.82 | 18.31% |
| | | 60 | 1.0–4.0 | 0 | 2.26 | 6.17 | 3.64 | 14.60% | −0.0651 | −1.16 | −5.66 | −12.92 | 21.61% |
| | | 70 | 1.0–4.0 | 0.0286 | 2.24 | 5.26 | 3.10 | 14.40% | −0.190 | −0.362 | −6.70 | −11.50 | 23.45% |
| | 9–63 | 30 | 0.5–4.0 | −0.0080 | 1.50 | 9.95 | 12.84 | 12.02% | 0 | −1.03 | −8.96 | −16.29 | 13.63% |
| | | 40 | 0.5–4.0 | −0.0181 | 1.96 | 9.57 | 5.64 | 10.41% | 0.0326 | −1.99 | −4.01 | −19.25 | 14.88% |
| | | 50 | 0.5–4.0 | −0.0661 | 2.88 | 6.61 | 5.47 | 11.18% | 0 | −1.71 | −5.43 | −16.14 | 17.47% |
| | | 60 | 1.0–4.0 | −0.0253 | 2.75 | 6.74 | 4.20 | 11.37% | −0.0663 | −1.42 | −5.40 | −16.25 | 16.94% |
| | | 70 | 1.0–4.0 | −0.122 | 3.61 | 4.98 | 4.18 | 13.28% | −0.0175 | −1.86 | −4.43 | −16.83 | 21.04% |
| $4.0 \leq \varepsilon_r \leq 5.0$ | 4–8 | 30 | 0.5–4.0 | 0.009 | 1.09 | 12.24 | 2.20 | 17.26% | 0.0153 | −1.31 | −4.84 | −13.81 | 13.90% |
| | | 40 | 0.5–4.0 | 0.0190 | 1.52 | 9.34 | 3.43 | 13.97% | 0.0342 | −1.68 | −3.85 | −12.36 | 12.32% |
| | | 50 | 0.5–4.0 | −0.0437 | 2.65 | 6.00 | 4.19 | 13.60% | −0.0403 | −1.16 | −5.18 | −11.75 | 23.20% |
| | | 60 | 1.0–4.0 | −0.0953 | 3.24 | 4.54 | 3.90 | 13.59% | −0.160 | −0.585 | −5.81 | −10.94 | 20.40% |
| | | 70 | 1.0–4.0 | 0.116 | 2.06 | 5.65 | 2.85 | 19.21% | −0.542 | 1.45 | −8.42 | −9.58 | 25.47% |
| | 9–63 | 30 | 0.5–4.0 | 0 | 1.36 | 12.34 | 5.04 | 19.00% | −0.0262 | −0.570 | −9.37 | −11.38 | 18.42% |
| | | 40 | 0.5–4.0 | −0.0307 | 2.50 | 8.83 | 5.69 | 16.15% | 0 | −1.48 | −5.64 | −14.80 | 15.35% |
| | | 50 | 0.5–4.0 | −0.0599 | 3.05 | 8.03 | 4.17 | 14.15% | 0.0736 | −2.64 | −2.14 | −17.39 | 24.86% |
| | | 60 | 1.0–4.0 | −0.126 | 3.89 | 5.37 | 4.71 | 12.40% | −0.111 | −1.44 | −3.93 | −16.52 | 21.43% |
| | | 70 | 1.0–4.0 | −0.0583 | 3.87 | 5.21 | 4.01 | 13.71% | −0.162 | −1.18 | −4.43 | −16.55 | 28.80% |

*The deviation within each applicable range is determined by comparing the predicted crosstalk of this work with the results of Ansoft's 2D Extractors.

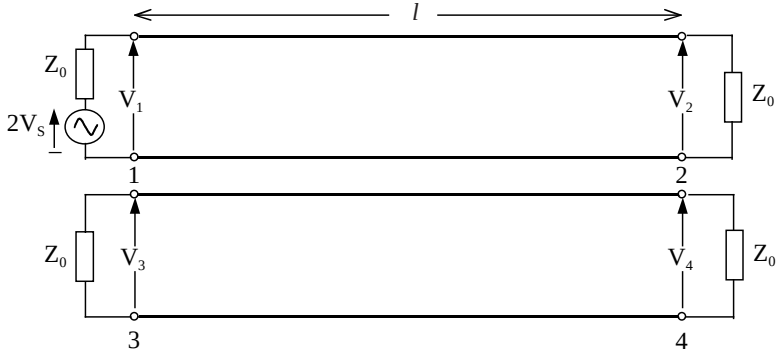


**Figure 3.** A pair of parallel-coupled transmission lines.

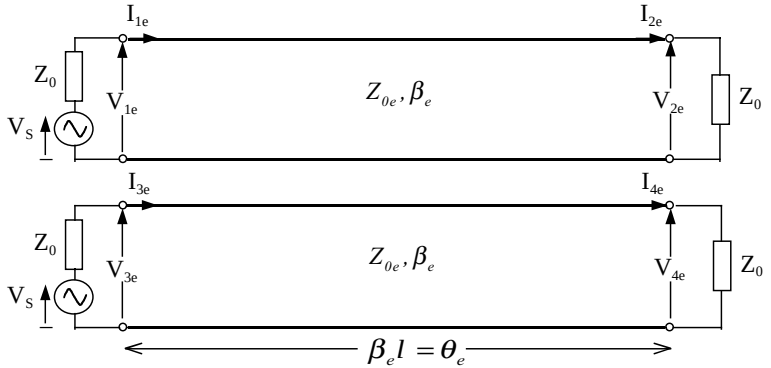


(a) Even-mode

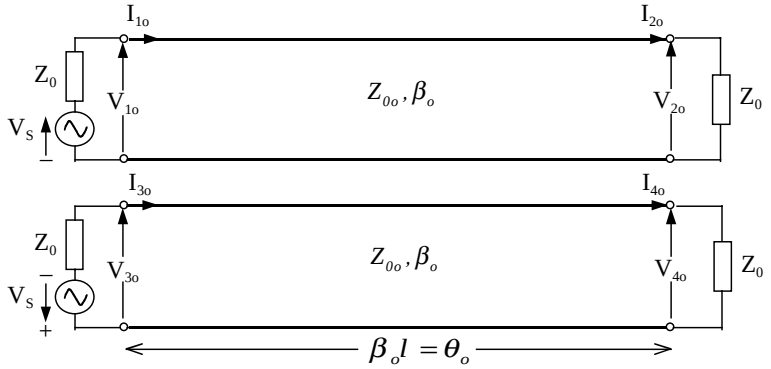


(b) Odd-mode

**Figure 4.** Separated even- and odd-mode equivalent circuits for the parallel-coupled lines.

phase constant $j\beta$ only. Since the structure is physically symmetrical, it can be seen that only two out of the four circuits actually need to be solved. Reference [8] gave a discussion on the even- and odd-mode wave properties for coupled lines totally embedded in a uniform dielectric. Mathematical expressions given in the following discussion are modified from those provided in Reference [8].

The total voltages and currents on the original structure are a superposition of the even- and odd-mode solutions as follows:

$$V_1 = V_{1e} + V_{1o} \qquad I_1 = I_{1e} + I_{1o} \tag{11a}$$
$$V_2 = V_{2e} + V_{2o} \qquad I_2 = I_{2e} + I_{2o} \tag{11b}$$
$$V_3 = V_{1e} - V_{1o} \qquad I_3 = I_{1e} - I_{1o} \tag{11c}$$
$$V_4 = V_{2e} - V_{2o} \qquad I_4 = I_{2e} - I_{2o} \tag{11d}$$

The $ABCD$ matrix for a transmission line can be used to express the voltage-current relations in phasor form as follows:

$$\begin{bmatrix} V_{1e} \\ I_{1e} \end{bmatrix} = \begin{bmatrix} \cos\theta_e & jZ_{0e}\sin\theta_e \\ jY_{0e}\sin\theta_e & \cos\theta_e \end{bmatrix} \begin{bmatrix} V_{2e} \\ I_{2e} \end{bmatrix} \tag{12a}$$

and

$$\begin{bmatrix} V_{1o} \\ I_{1o} \end{bmatrix} = \begin{bmatrix} \cos\theta_o & jZ_{0o}\sin\theta_o \\ jY_{0o}\sin\theta_o & \cos\theta_o \end{bmatrix} \begin{bmatrix} V_{2o} \\ I_{2o} \end{bmatrix} \tag{12b}$$

where $\theta_e = \beta_e l$ and $\theta_o = \beta_o l$.

The terminal conditions are given by:

$$V_{1e} + I_{1e}Z_0 = V_s \tag{13a}$$
$$V_{1o} + I_{1o}Z_0 = V_s \tag{13b}$$
$$V_{2e} = Z_0 I_{2e} \tag{13c}$$
$$V_{2o} = Z_0 I_{2o} \tag{13d}$$

All the terminal voltage and current components can be obtained by solving Equations (12) and (13) simultaneously.

Consider a case where the source is a $2V_s$ step input with rise time $T_r$. This transient signal can be decomposed into a series of Fourier components. The overall induced far-end crosstalk can be obtained by superposition the response caused by each of the frequency component. In an inhomogeneous medium, the odd-mode signal travels faster than the even-mode signal. If the rise time of the driving signal is less than the time difference between the even- and odd-mode delay, the far-end crosstalk reaches its saturation value [9]. Since the odd-mode signal reaches the far-end faster than the even-mode signal, expression (11d) implies that the far-end saturation voltage is equal to the odd-mode

voltage $V_{2o}$, which is given as:

$$V_{2o} = \frac{Z_0 Z_{0o} V_i}{2Z_{0o} Z_0 \cos\theta_o + j(Z_{0o}^2 + Z_0^2)\sin\theta_o} \tag{14}$$

where $V_i$ is the amplitude of Fourier component.

For loosely coupled lines, $Z_{0o} \approx Z_0$, thus the magnitude of $V_{2o} \approx V_i/2$. Assuming all the odd-mode Fourier components travel at the same velocity, the overall far-end saturation voltage will be $V_s/2$, i.e., half of the magnitude of the driving signal enters the active line.

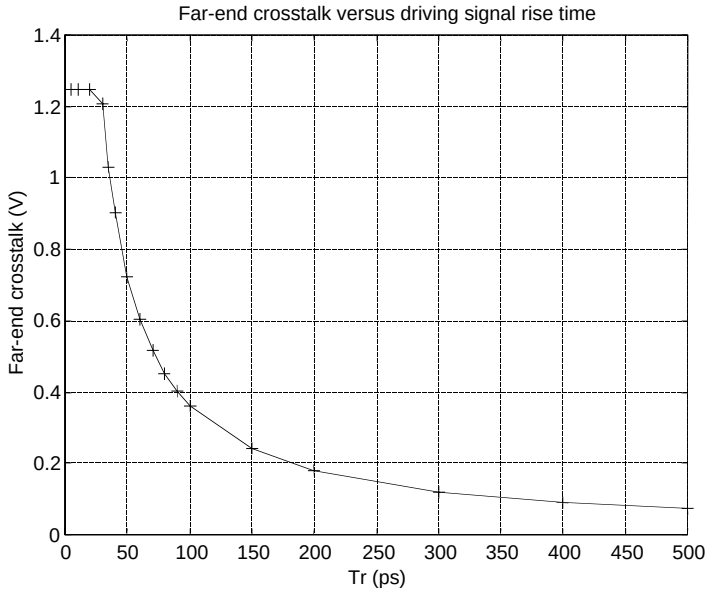


**Figure 5.** Saturation of the far-end crosstalk.

The far-end saturation voltages for a few pairs of coupled lines with arbitrary parameters were studied using Maxwell Spicelink. The results obtained further verified the above phenomenon. One of the example is given in Figure 5, where the line parameters are $W = 7$ mils, $H = 4$ mils, $S = 14$ mils, $l = 15$ cm, $\varepsilon_r = 4.4$, and the source is 5 V step voltage with a source impedance equal to the characteristic impedance. The time difference between the even- and odd-mode delay is calculated to be about 43 ps using 2D/3D Extractors. It can be observed that when the rise time $< 40$ ps, the far-end crosstalk saturates at about 1.25 V, i.e., half of the amplitude of the driving signal enters the active line.

In fact, for sub-pico signal rise time, conductor and dielectric losses, and dispersion effect are not negligible. The far-end saturation voltage will be lower than that of the lossless and dispersionless case. Nevertheless, the saturation value in the lossless case serves as an upper bound for the far-end crosstalk, so as to complement the derived lossless far-end expression which does not take the saturation into account.

## 4. THE EFFECT OF LOSSES AND DISPERSION ON CROSSTALK NOISE

The proposed expressions in (3) and (4) are only applicable to lossless and dispersionless cases. Both losses and dispersion effect will cause attenuation and distortion to signal. Attenuation will cause the amplitude of the signal to decrease while dispersion effect significantly degrades the signal rise time (steepness) as it propagates down the line [10].

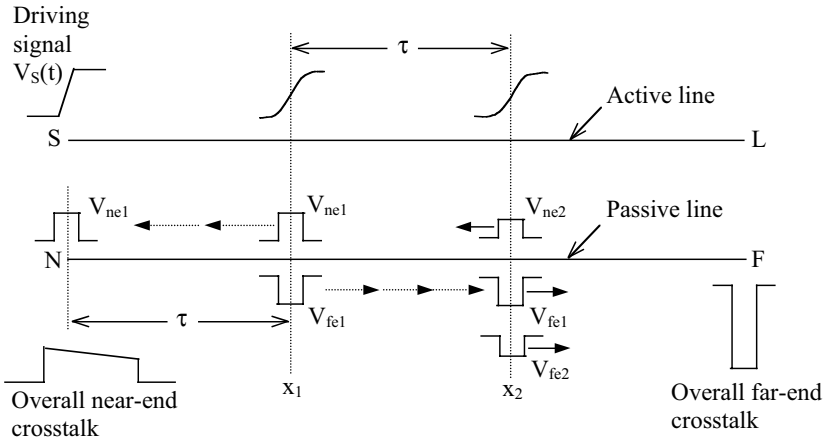


**Figure 6.** Mechanism of inducing the near-end and far-end crosstalk.

Since the near-end and far-end crosstalk depend on the amplitude and time derivative of the driving signal respectively, the amplitude of the induced crosstalk pulses are smaller at location farther from the terminal $N$ (i.e., $V_{ne2} < V_{ne1}$ and $V_{fe2} < V_{fe1}$), as depicted in Figure 6. Consequently, the resultant overall near-end crosstalk waveform will have diminishing amplitude. Nevertheless, the derived near-end crosstalk expression based on lossless and dispersionless assumption can still predict the initial amplitude of the near-end

crosstalk accurately. Since the maximum crosstalk amplitude is of the most interest, it does not worth the trouble to modify the near-end crosstalk expression merely to account for the diminishing amplitude.

On the other hand, the overall far-end crosstalk will be much smaller as compared to the lossless and dispersionless case. The seriousness of signal distortion must then be investigated if an accurate prediction of the far-end crosstalk is required.

### 4.1. The Valid Frequency Range for Lossless and Dispersionless Assumption

The applicable frequency range for far-end crosstalk expression in Equation (4) is investigated in this section. The frequency range where lossless and dispersionless assumption is valid depends on a few factors. Strictly speaking, the conductor loss starts to increase after the break frequency [11]. Since most PCB traces are made of copper with high conductivity values, the ohmic loss can be neglected most of the time [12]. Also, the conductor loss tends to be very small because the current flowing along the line is small as the characteristic impedance of the line is very large compared to the digital voltage applied between the strip and ground plane [10]. While for most of the dielectrics, their losses are several orders of magnitude less than unity up to the lower gigahertz range. Practically, the dielectric losses are negligible below 1 GHz so that the lossless assumption can be accepted most of the time [2].

Also, the dispersion effect is not significant for frequencies in lower gigahertz region [8]. Since dispersion effect is the main culprit that causes signal rise time degradation [10], which results in smaller induced far-end crosstalk voltage, it becomes the dominant factor that affects accuracy in far-end crosstalk prediction. Therefore the derived far-end crosstalk expressions based on lossless and dispersionless assumption can be used with reasonable accuracy up to 1 GHz.

For digital signal, the frequency spectral rolls off at $-20$ dB/decade up to "knee frequency" [2], which is given by:

$$f_{knee} = \frac{0.5}{T_{edge}} \tag{15}$$

where $T_{edge}$ is the edge rates (use the fastest value of either the rise or fall times). With an edge rate of 500 ps, Equation (15) gives $f_{knee} = 1$ GHz. Thus, for any digital signal with edge rates larger than 500 ps, the lossless and dispersionless assumption is acceptable and the signal experiences negligible degradation. Therefore, the derived far-end crosstalk expressions in (4) can be applied for any digital signals

with edge rates $\geq$ 500 ps, or any other input signal that contains significant spectrum up to 1 GHz only.

### 4.2. Incorporation of Losses and Dispersion Effect in Far-end Crosstalk Prediction

For significant harmonic frequency $> 1$ GHz, the effect of both losses and dispersion on the far-end crosstalk levels is accounted for by investigating the gradient of the distorted driving signal. The peak far-end crosstalk levels can be then predicted by modifying the time derivative term in the lossless expression in (4).

The analysis of transient signal degradation is based on the following assumptions:

- The driving signal travels down the active line does not degrade due to the presence of adjacent line (loosely coupled lines). The degradation of the driving signal is merely caused by the losses and dispersion effect of the active line itself;
- The induced crosstalk signals that propagate on the passive line experience negligible distortion and attenuation;
- Radiation loss is not considered because it is significant only in microstrip lines with discontinuities.

The effects of conductor and dielectric losses are not studied separately but they are summed together as a single attenuation constant:

$$\alpha(\omega) = \alpha_c(\omega) + \alpha_d(\omega) \tag{16a}$$

where $\alpha_c(\omega)$ and $\alpha_d(\omega)$ represent the conductor and dielectric losses respectively. The losses can be treated by the following expressions [13]:

$$\alpha_c = 1.6 \left[ \frac{0.072\sqrt{f}}{8.68 W Z_0} \right] \qquad \text{(nepers/unit length)} \tag{16b}$$

where $f$ is in GHz, $Z_0$ is in ohms, $W$ is in m and factor 1.6 is used to account for surface roughness (assuming the r.m.s. surface roughness to be of similar magnitude compared to the skin depth); and

$$\alpha_d = \pi \cdot \frac{\varepsilon_r}{\sqrt{\varepsilon_{reff}(0)}} \cdot \frac{\varepsilon_{reff}(0) - 1}{\varepsilon_r - 1} \cdot \frac{\tan\delta}{\lambda_0} \quad \text{(nepers/unit length)} \tag{16c}$$

where

| | | |
|---|---|---|
| $\varepsilon_r$ | – | relative dielectric constant of the substrate, |
| $\varepsilon_{reff}$ | – | effective dielectric constant at $f = 0$, which can be approximated by Equation (6), |
| $\lambda_0$ | – | free-space wavelength, |
| $\tan\delta$ | – | loss tangent of the substrate. |

The loss tangent here is assumed to be constant with frequency. The effective dielectric constant, $\varepsilon_{reff}(f)$, which accounts for dispersive distortion can be calculated by the following expressions, with frequency $f$ in GHz and thickness $H$ in cm [14]:

$$\varepsilon_{reff}(f) = \varepsilon_r - \frac{\varepsilon_r - \varepsilon_{reff}(0)}{1 + P(f)} \tag{17a}$$

and the form of the denominator frequency function is

$$P(f) = P_1 P_2 \{(0.1844 + P_3 P_4) 10 f H\}^{1.5763} \tag{17b}$$

where

$$\left.\begin{aligned} P_1 &= 0.27488 + \{0.6315 + 0.525/(1 + 0.157 f H)^{20}\} \cdot (W/H) \\ &\quad -0.065683 \exp(-8.7513 W/H) \\ P_2 &= 0.33622\{1 - \exp(-0.03442 \varepsilon_r)\} \\ P_3 &= 0.0363 \exp(-4.6 W/H) \cdot [1 - \exp\{-(f H/3.87)^{4.97}\}] \\ P_4 &= 1 + 2.751[1 - \exp\{-(\varepsilon_r/15.916)^8\}] \end{aligned}\right\} \tag{17c}$$

The applicable range is very wide:

$$1 \le \varepsilon_r \le 20, \quad 0.1 \le W/H \le 100, \quad 0 \le H/\lambda_0 \le 0.13$$

The computations for the distorted waveforms at a distance $l$ along a microstrip line are made using:

$$V(t, z = l) = \frac{1}{2\pi} \int_{-\infty}^{+\infty} V(\omega, z = 0) e^{j\omega t - \gamma(\omega) l} d\omega \tag{18a}$$

where

$$\gamma(\omega) = \alpha(\omega) + j\beta(\omega) \tag{18b}$$

$$\beta(\omega) = \frac{\omega}{c} \sqrt{\varepsilon_{reff}(f)} \tag{18c}$$

and $V(\omega, z = 0)$ is the Fourier transform of the pulse at the reference point ($l = 0$) of the line.

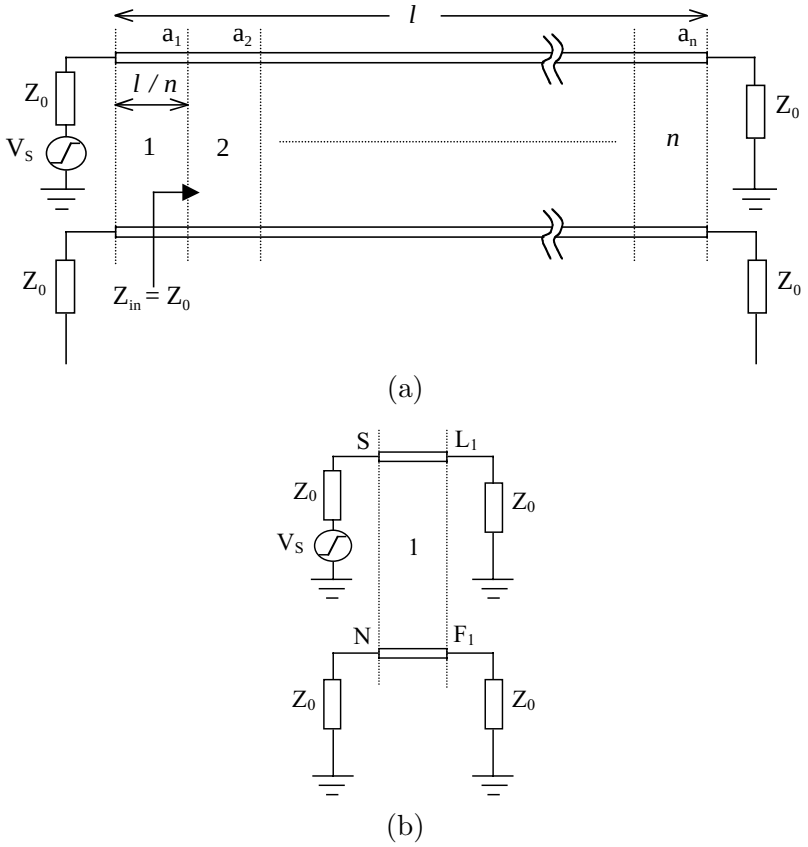


**Figure 7.** (a) A pair of coupled microstrip lines, and (b) the equivalent circuit of the first segment.

Consider a pair of coupled microstrip lines as shown in Figure 7a. The coupled lines are divided into $n$ equal length segments. Since both lines are terminated in their characteristic impedance $Z_0$, the input impedance at any point looking towards the end of the line is equivalent to $Z_0$. Therefore, the equivalent circuit of segment 1 is as shown in Figure 7b. Assuming the driving signal does not degrade much as it propagates along the first segment, the lossless and dispersionless far-end crosstalk expression in (4) can be used to approximate the far-end crosstalk induced at terminal $F_1$ in Figure 7b.

The waveform of the driving signal $V_s$ at the end point of segment 1 (i.e., point $a_1$ in Figure 7a) can be determined using Equation (18). The degraded driving signal waveform at point $a_1$ can be thought as

a new driving signal that applied to segment 2. The equivalent circuit for Segment 2 is the same as that for Segment 1 (Figure 7b). Similarly the far-end crosstalk at the end of segment 2 can be approximated using expression in (4). Simultaneously, the far-end crosstalk induced at the end of segment 1 has also propagated to the end of segment 2. Therefore, both far-end crosstalk waveforms appear at the end of segment 2 at the same instant of time and add in-phase. The same explanation goes for other segment until $V_s$ arrives at the receiving end of the active line. The overall far-end crosstalk amplitude will be the sum of each individual far-end crosstalk induced in every segment:

$$V_{fe}\Big|_{overall} = K_f \cdot \frac{T_p}{n} \cdot \sum_{i=0}^{n-1} \left(\frac{dV_s}{dt}\right)_i \tag{19}$$

where $\left(\frac{dV_s}{dt}\right)_i$ is the time derivative of the degraded driving signal determined using Equation (18) at initial point of segment $i+1$.

If $n$ is large enough such that the length of each segment is much smaller than the overall coupled length $l$, the overall far-end crosstalk value will converge ($n = 100$ will be sufficient for this purpose).

Nevertheless this is a time consuming process where the degraded waveforms at the end point of every segment need to be determined. Another approximate approach can be used to simplify the process, where it assumes the driving signal $V_s$ degrades linearly along the active line. With this assumption, we only need to find the time derivative of the degraded driving signal waveform at the output of the active line, and the time derivative at initial point of any segment can be determined as:

$$\left(\frac{dV_s}{dt}\right)_i = \left(\frac{dV_s}{dt}\right)_0 - \frac{i}{n} \cdot \left\{\left(\frac{dV_s}{dt}\right)_0 - \left(\frac{dV_s}{dt}\right)_n\right\}, \quad 0 < i < n \tag{20}$$

where

$\left(\frac{dV_s}{dt}\right)_0$ is the time derivative of undegraded $V_s$ at the input of the active line;

$\left(\frac{dV_s}{dt}\right)_n$ is the time derivative of degraded $V_s$ at the output of the active line.

Combining Equations (19) and (20) gives:

$$V_{fe}\Big|_{overall} = K_f \cdot T_p \cdot \left(\frac{dV_s}{dt}\right)_{equivalent} \tag{21a}$$

where

$$\left(\frac{dV_s}{dt}\right)_{equivalent} = \frac{1}{n} \cdot \sum_{i=0}^{n-1} \left[ \left(\frac{dV_s}{dt}\right)_0 - \frac{i}{n} \cdot \left\{ \left(\frac{dV_s}{dt}\right)_0 - \left(\frac{dV_s}{dt}\right)_n \right\} \right] \tag{21b}$$

## 5. PROCEDURE FOR PREDICTION OF CROSSTALK

The following describes the steps involved in applying the derived expressions to predict near-end and far-end crosstalk for a given coupled microstrip lines configuration:

1. Find $T_p$ using Equations (6) and (7).
2. Use equation below to approximate the characteristic impedance of the line:
$$Z_0 = \frac{377 \left[ \frac{W}{H} + 1.98 \cdot \left(\frac{W}{H}\right)^{0.172} \right]^{-1}}{\sqrt{\varepsilon_{eff}}} \tag{22}$$
which is accurate to $< 0.3\%$ for all $(W/H) > 0.06$ [7].
3. Based on $\varepsilon_r$, $H$ and the calculated $Z_0$ above, choose the correct set of polynomial coefficients from the look-up Table 1.
4. For any frequency, apply expression in (3) to calculate the near-end crosstalk. For signal with significant harmonic frequency $\leq 1\,\text{GHz}$ or for digital trapezoidal signal with edge rate ($T_{rise}$ or $T_{fall}$) $\geq 500\,\text{ps}$, apply expression in (4) to calculate the far-end crosstalk values directly. For signal with significant harmonic frequency $> 1\,\text{GHz}$ or for digital trapezoidal signal with edge rate ($T_{rise}$ or $T_{fall}$) $< 500\,\text{ps}$, apply Equation (21) to approximate the amplitude of far-end crosstalk. For either case, if the predicted far-end crosstalk is larger than half of the magnitude of the driving signal entering the active line, this implies that saturation has occurred. Thus the far-end crosstalk is equal to half of the magnitude of the driving signal entering the active line.

## 6. COMPARISONS WITH RESULTS FROM FIELD SOLVER AND OTHER MODELS

The predicted crosstalk of this work is compared with those of Ansoft's Maxwell Spicelink and Agilent's ADS, and results available from the open literature. As the first application example, the crosstalk on a PCBs constructed on $\varepsilon_r = 4.8$ substrate with the following parameters are investigated [3]: $W = 15\,\text{mils}$, $H = 8\,\text{mils}$, $T = 1.37\,\text{mil}$, coupled

length $l = 10''$. The input signal is a $5V_{p-p}$ pulse with 1 ns rise time. Figures 8a–8b show the peak near-end and far-end crosstalk levels versus $S/W = 0.5$ to 4.0, as compared to the results predicted by Reference [3], and those simulated using commercial field solvers (Maxwell Spicelink and ADS). It can be observed that the results of this work match well with the field solver results in all cases.

The next example investigates crosstalk on coupled lines with $W = 7$ mils, $H = 4$ mils, $T = 1.38$ mil (1 ounce), coupled length $l = 20$ cm, $\varepsilon_r = 3.9$ (BT), and the input signal is a 5 V digital signal with 500 ps rise time. Figures 9a–9b show the peak near-end and far-end crosstalk levels versus $S/W$ respectively. Comparison of the results again shows good agreement. The results show that the proposed expressions predict crosstalk with great accuracy.

## 7. COMPARISONS WITH MEASUREMENT RESULTS

Parallel-coupled copper microstrip lines with 1 ounce thickness are constructed on FR4 ($\varepsilon_r = 4.8$) printed circuit board with substrate thickness $H = 1.6$ mm. To obtain 50 Ω characteristic impedance, the width $W$ of the line is set to 3 mm. Six pairs of $9''$ coupled lines with separation distance $S$ at $0.5W$, $1.0W$, $1.5W$, $2.0W$, $2.5W$ and $3.0W$ are constructed. Four pairs of parallel lines separated at $S = 1.0W$ with $3''$, $5''$, $7''$ and $9''$ coupled lengths are also constructed. The near-end and far-end crosstalk on the victim line are measured using Tektronix TDS8000 digital sampling oscilloscope with 80E04 sampling module.

The driving signal $V_s$ applied to the line is an 80 MHz trapezoidal waveform with 1 V amplitude and about 2 ns rise time constructed using a crystal oscillator and an inverter. The maximum $dV_s/dt$ required for calculating the peak far-end noise voltage is determined by measuring the $\Delta V$ and $\Delta t$ of the driving signal. All line ends are terminated in 50 Ω, which match the characteristic impedance of a single line. Figures 10a–10b show the comparisons of the predicted peak near-end and far-end crosstalk with measured values for $9''$ coupled lines with respect to separation distance $S$. While Figure 10c shows the comparison of the predicted peak far-end crosstalk with measured values for different coupled lengths (separation between lines is fixed at $S = 1.0W$). The comparison of results demonstrates good agreement between the predicted values and the measurements. Table 2 gives the maximum and RMS deviations of the predicted crosstalk voltages from the measured values. The maximum deviations are lower than 13% in all cases.

Another crosstalk measurement on the physical board is performed with the internal TDR step generator of the oscilloscope used

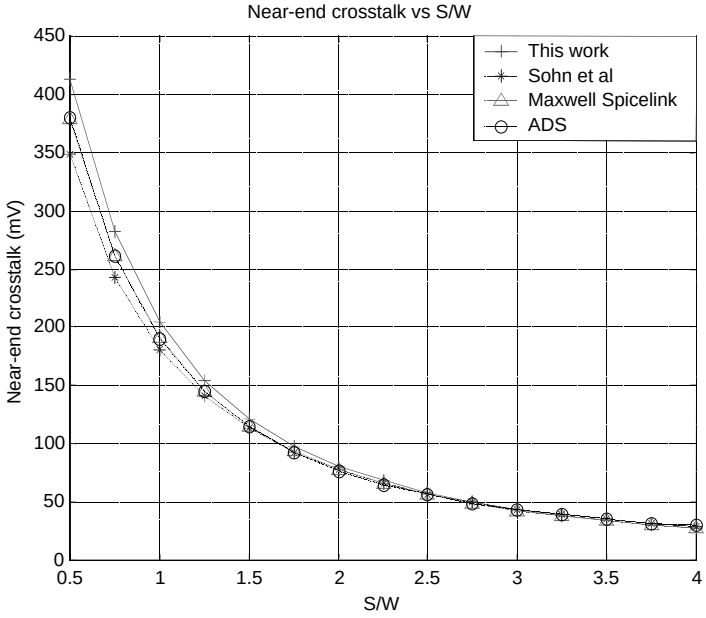


(a)

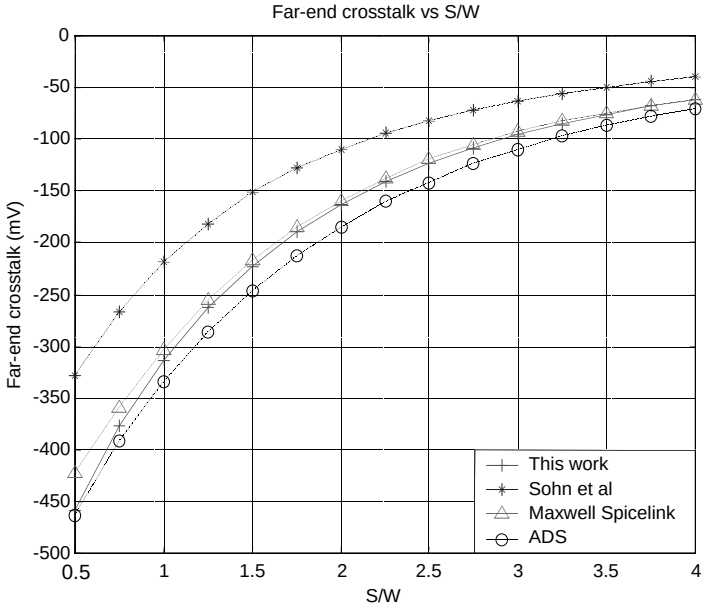


(b)

**Figure 8.** (a) Near-end crosstalk, and (b) far-end crosstalk.

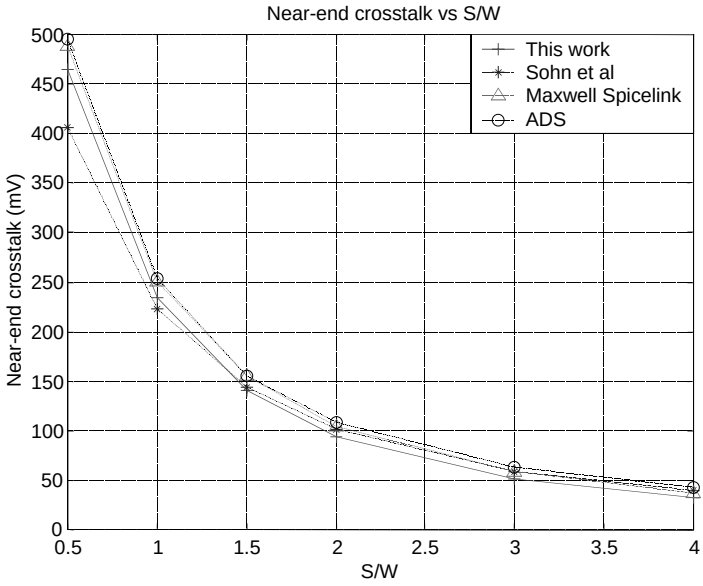


(a)

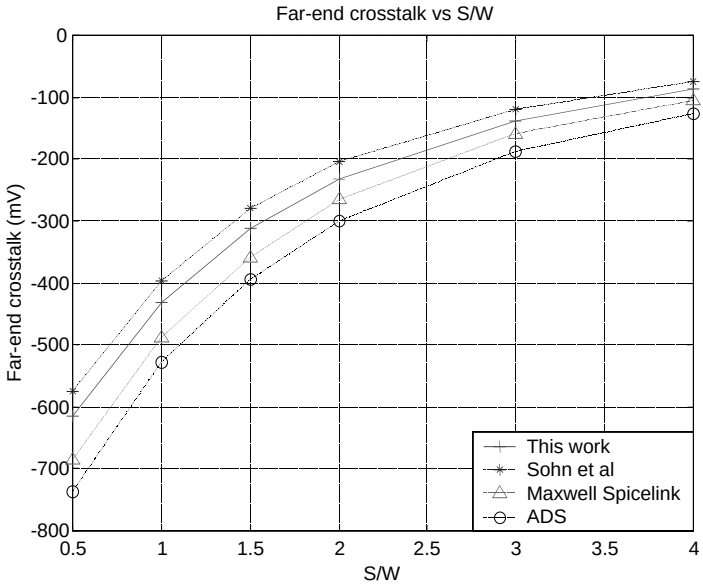


(b)

**Figure 9.** (a) Near-end crosstalk, and (b) far-end crosstalk.

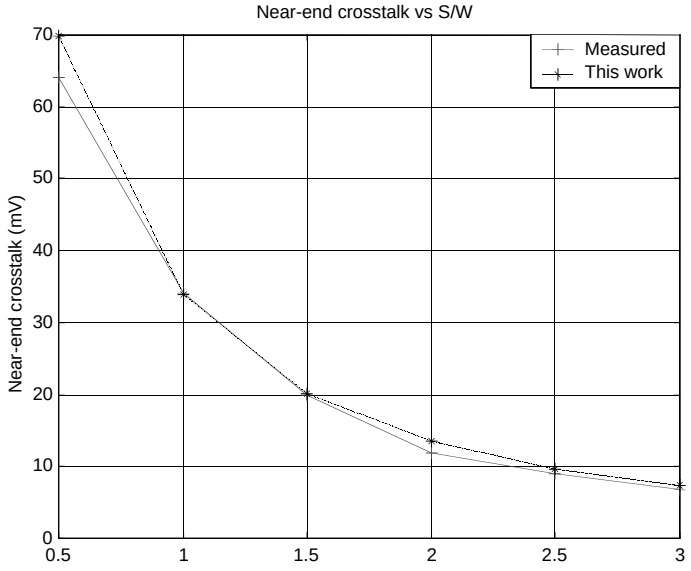


(a)

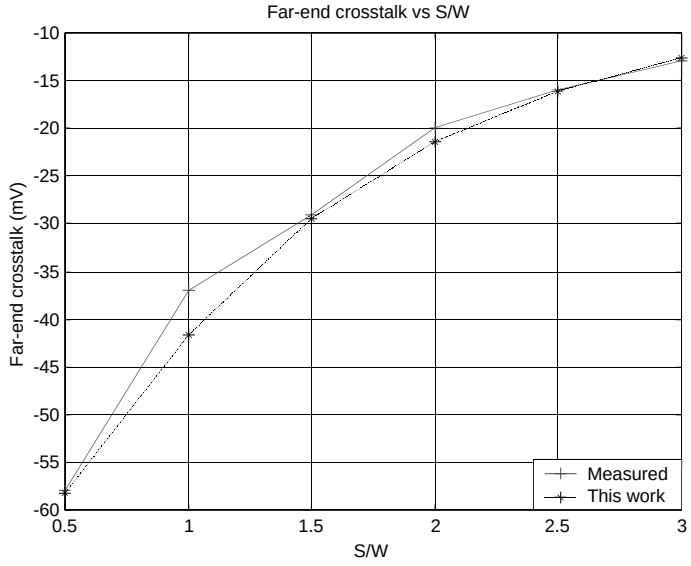


(b)

**Figure 10.** Comparison of measured and predicted (a) near-end crosstalk, (b) far-end crosstalk, and (c) far-end crosstalk for different coupled lengths.

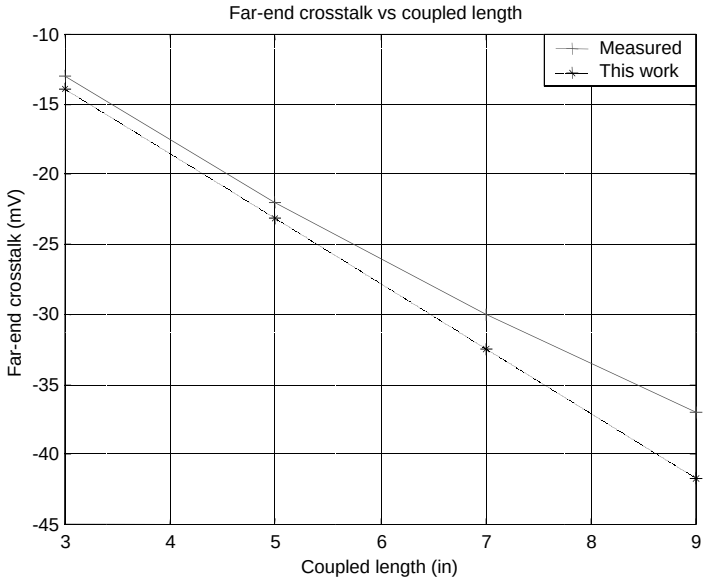


(c)

**Figure 10.** (cont'd)

**Table 2.** Deviation of predicted crosstalk from measured values.

| Deviation | Near-end crosstalk vs $S/W$ Figure 10a | Far-end crosstalk vs $S/W$ Figure 10b | Far-end crosstalk vs coupled length Figure 10c |
|---|---|---|---|
| Maximum (%) | 12.59 | 12.78 | 12.78 |
| RMS (%) | 8.02 | 6.22 | 7.17 |

as the signal source. The signal that enters the line has a step of 230 mV amplitude with about 100 ps rise time.

The near-end crosstalk is calculated using the derived expression directly and the comparison is shown in Figure 11. The maximum deviation is 25.32% while the RMS is 13.60%. This results show that the proposed expressions give good accuracy even for near-end crosstalk values as small as a few mV.

For far-end crosstalk, the method proposed in Section 4.2 should be used since the significant harmonic frequency is 5 GHz for 100 ps rise time. The loss tangent of the dielectric is 0.02 and is assumed to be constant with frequency. The degraded driving signal waveform at

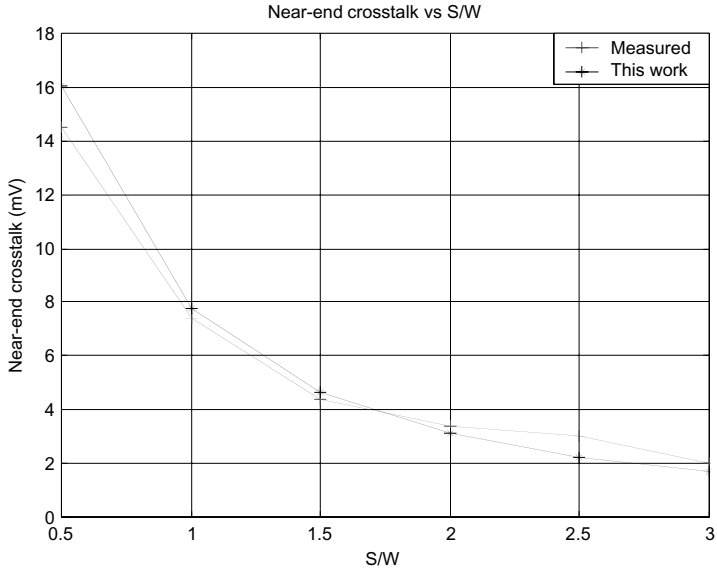


**Figure 11.** Comparison of measured and predicted near-end crosstalk.

the output of the active line is computed using Equation (18). The computed and measured waveforms are shown in Figures 12a and 12b respectively. The measured waveform has about 220 mV amplitude and 230 ps rise time, while the predicted waveform has about 230 mV amplitude and 200 ps rise time. Possible reason for the discrepancy is the assumption that the dielectric loss is frequency independent. Another important reason is discontinuities at interconnection between the traces and SMA type connectors can cause radiation loss.

To calculate the far-end crosstalk using Equation (21), the time derivative of the driving signal at the output of the active line is approximated as 150 mV/100 ps (see Figure 12a). Figure 13 depicts the comparisons of measured, our predicted values and those of ADS between lossless and dispersionless assumption with lossy and dispersion consideration. The observation discussed in Section 3 has been applied to obtain the saturation value of the far-end crosstalk (i.e., $V_s/2 = 230/2 = 115$ mV). It can be observed that inclusion of losses and dispersion effect gives results closer to the measured values and those of ADS, except at separation $S = 0.5W$. The large discrepancy at $S = 0.5W$ is due to saturation of the far-end crosstalk, where the saturation value is actually lower than $V_s/2 = 115$ mV due to losses and dispersion effect. However, this does not detract from the usefulness of the method because it is unnecessary to predict the

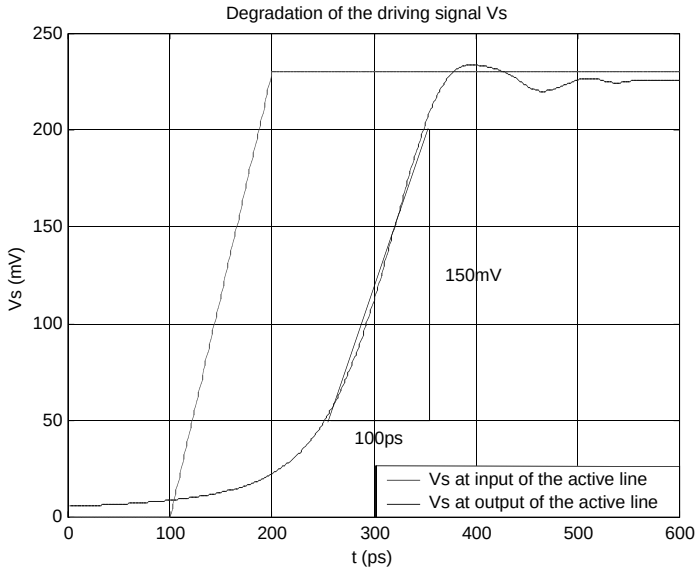


(a)

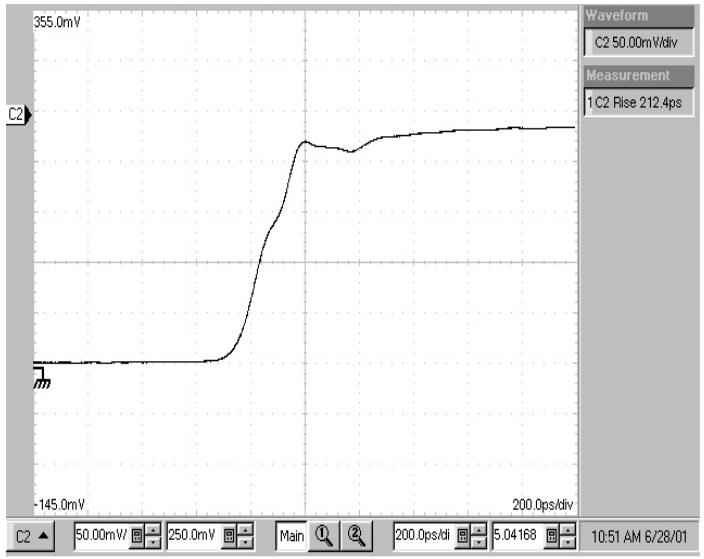


(b)

**Figure 12.** (a) Prediction of the driving signal distortion, and (b) measured driving signal waveform at the output of the active line.

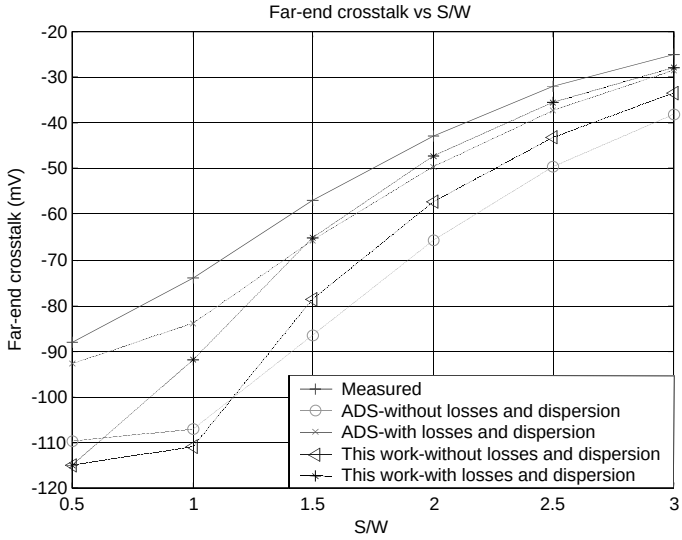


**Figure 13.** Comparison of measured and predicted far-end crosstalk versus separation with and without losses and dispersion effect.

saturation value accurately. This is because when saturation occurs, the far-end crosstalk noise will be too large for safe circuit operation and this implies that a greater spacing between the coupled lines should be imposed. In this case, for example, the measured far-end crosstalk is 88 mV, which is about 38% of the 230 mV driving signal. The rise time of the input signal should be greater than the time difference between the even- and odd-mode delay in order to avoid the far-end noise reaching its saturation value [9]. Table 3 shows the improvement of the maximum and RMS deviations from the measured values with inclusion of losses and dispersion effect. Similar approach is used to predict the far-end crosstalk for different coupled lengths (separation between the coupled lines is fixed at $S = 1.0W$). Figure 14 and Table 4 show the comparison of results and deviation analysis respectively. Again incorporation of losses and dispersion effect gives closer predicted results to the measurements. The maximum deviation is reduced from 49.94% to 24.12% and the RMS is reduced from 30.52% to 16.80%.

**Table 3.** Deviation of predicted far-end crosstalk versus separation and those of ADS from the measured values.

| Deviation | This work (without losses and dispersion) | This work (with losses and dispersion) | ADS (without losses and dispersion) | ADS (with losses and dispersion) |
|---|---|---|---|---|
| Maximum (%) | 49.94 | 30.68 | 55.41 | 16.75 |
| RMS (%) | 37.20 | 18.59 | 48.22 | 13.92 |

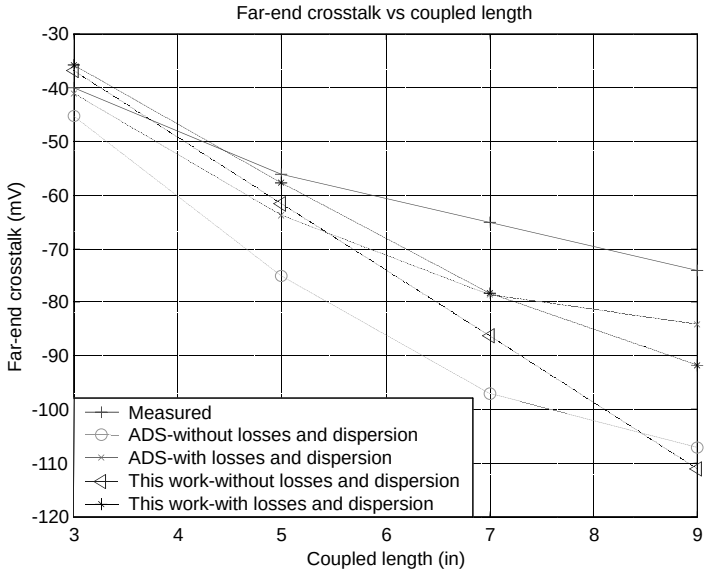


**Figure 14.** Comparison of measured and predicted far-end crosstalk versus coupled length with and without losses and dispersion effect.

**Table 4.** Deviation of predicted far-end crosstalk versus coupled length and those of ADS from the measured values.

| Deviation | This work (without losses and dispersion) | This work (with losses and dispersion) | ADS (without losses and dispersion) | ADS (with losses and dispersion) |
|---|---|---|---|---|
| Maximum (%) | 49.94 | 24.12 | 49.26 | 14.31 |
| RMS (%) | 30.52 | 16.80 | 38.03 | 20.74 |

## 8. CONCLUSION

As compared to other approaches, the proposed crosstalk expressions in this paper for lossless and dispersionless case are simple and suitable for hand calculations. The derived near-end expression gives accurate peak noise prediction for any frequency while the far-end expression is valid up to 1 GHz. The design and layout engineers can use the derived expressions to establish design guidelines for determining the safe separation between coupled microstrip lines for a given maximum allowable crosstalk. Saturation of far-end crosstalk has also been investigated mathematically from the point view of the even- and odd-mode wave properties. It is proved that the far-end crosstalk saturates at half of the magnitude of the driving signal enters the active line in lossless case. The far-end saturation voltage will be, of course, lower in lossy and dispersive case. However, the saturation value in lossless case can serve as an upper bound for the far-end crosstalk. The effect of losses and dispersion on crosstalk noise was also discussed in detail for cases with harmonic frequency $> 1$ GHz. Frequency-dependent conductor loss and dispersion effect, and frequency-independent dielectric loss are incorporated into the far-end crosstalk analysis by means of investigating the gradient of the distorted driving signal.

The predicted crosstalk values match reasonably well with those of measurements, commercial field solvers and results available in literature. Although the examples given are based on digital signal, the proposed methods are applicable for any type of input signals.

## REFERENCES

1. Feller, A., H. R. Kaupp, and J. J. Digiacoma, "Crosstalk and reflections in high-speed digital systems," *Fall Joint Computer Conf. Proceeding*, 511–525, 1965.
2. Johnson, H. W. and M. Graham, *High-Speed Digital Design: A Handbook of Black Magic*, Prentice Hall, 1993.
3. Sohn, Y. S., J. C. Lee, H. J. Park, and S. I. Cho, "Empirical equations for electrical parameters of coupled microstrip lines with one side exposed to air," *IEE Electronics Letters*, Vol. 35, No. 11, 906–907, 1999.
4. Montrose, M. I., *Printed Circuit Board Design Techniques for EMC Compliance*, 2nd Edition, IEEE Press, 2000.
5. Chang, C. S., "An overview of computer packaging architecture and electrical design," *Southern Tier Technical Conf.*, 239–257, 1990.

6. Sengupta, M., S. Lipa, P. Franzon, and M. Steer, "Crosstalk driven routing advice," *Electronic Components and Technology Conf.*, 687–694, 1994.
7. Ramo, S., J. R. Whinnery, and T. Van Duzer, *Fields and Waves in Communication Electronics*, John Wiley & Sons, 1993.
8. Edwards, T., *Foundations for Microstrip Circuit Design*, 2nd Edition, John Wiley & Sons, 1998.
9. Agrawal, A. P., C. S. Chang, and D. A. Gernhart, "Design considerations for digital circuit interconnections in a multilayer printed circuit board," *IEEE International Conf. on Computer Design: VLSI in Computers and Processors*, 472–478, 1991.
10. Leung, T. and C. A. Balanis, "Attenuation distortion of transient signals in microstrip," *IEEE Trans. on Microwave Theory Tech.*, Vol. 36, No. 4, 765–768, 1988.
11. Roden, J. A., C. R. Paul, W. T. Smith, and S. D. Gedney, "Finite-difference, time-domain analysis of lossy transmission lines," *IEEE Trans. on Electromagnetic Compatibility*, Vol. 38, No. 1, 15–24, 1996.
12. Kung, F. W. L. and H. T. Chuah, "System modeling of high-speed digital printed circuit board using SPICE," *Progress in Electromagnetics Research*, Vol. 20, 179–212, 1998.
13. Hammerstad, E. O. and F. Bekkadal, "A microstrip handbook," *ELAB Report*, 98–110, University of Trondheim, Norway, 1975.
14. Kirschning, M. and R. H. Jansen, "Accurate model for effective dielectric constant of microstrip with validity up to milimetre-wave frequencies," *IEE Electronics Letters*, 272–273, 1982.